KRONOS FUSION ENERGY

PAPER 2.104 · THE KRONOS 2026 SERIES

Operating the Consumable Centrepost of a Compact Spherical-Tokamak Breeder: Demountable-Cartridge Swap Logistics, Fleet RAMI, and Centrepost Radial-Budget Reconciliation

The Hyperion breeder is built around a consumable centrepost: a demountable high-temperature-superconductor column that is periodically swapped rather than designed to survive the...

Read it live — 3-D model · physics validator · film series

BY P I FORD

2026 · EDITORIAL EDITION

THE OFFICIAL RECORD

What this document is, and how to read its numbers

This is a combined editorial. It gathers, in one volume, the two design studies Kronos Fusion Energy released in 2026 — a compact spherical-tokamak tritium/helium-3 breeder and a deuterium–helium-3 tandem-mirror generator — together with the intellectual-property estate, the people, and, in the internal edition, the full commercial case. The scientific text is the same text that appears in the arXiv preprints and the journal submissions; the editorial adds the apparatus a reader needs to hold the whole program at once, and nothing in the physics is altered to fit it.

THE HONESTY STANCE IS THE ASSET

Every headline quantity carries an **evidence class** — DERIVED RECOMPUTED MEASURED REQUIREMENT — and, where a number is a modelled extrapolation rather than a demonstrated value, it is labelled as such and its downside is shown next to it. Several quantities in the underlying corpus moved after first publication; where a value has been withdrawn or restated, the record says so plainly. This is deliberate: a diligence team will find the load-bearing assumptions, so the document surfaces them first.

TWO EDITIONS

This volume is issued in two editions. The **public edition** (light) carries the physics and the design only — no dollar, price, or per-kilogram figure appears anywhere in it. The **internal edition** (dark) adds the economics, the funding architecture, and the defense-commercial analysis, and is marked *Confidential* accordingly; it is not for public distribution. Where the commercial case rests on a modelled assumption rather than a demonstrated one, it is labelled as such and its downside is shown alongside it, on the same terms as the physics.

TITLE	The Kronos Fleet — Hyperion · Aegis · MetroVolt: A Combined Design & Commercialization Study
AUTHOR	Priyanca Ford, Founder & CEO, on behalf of Kronos Fusion Energy
EDITION	2026 Combined Editorial · first issue
COMPANION WORKS	The five-paper arXiv drop — (1) Breeder, (2) Burner, (3) REBCO magnet & tape, (4) Direct Energy Conversion, (5) AI/ML/Quantum control — with matching numbered Zenodo deposits, plus the IOP journal and IAEA-FEC submissions. Patents were filed before the drop.
NAMING	Hyperion = the breeder; Aegis (defense) and MetroVolt (data-center) = one generator in two housings. Internal mode letters (D1, L) do not appear on public surfaces.
STATUS	Conceptual design & simulation study. Nothing herein is a construction commitment.

HOW TO READ THIS VOLUME

The fleet at a glance, and the way its numbers are marked

This volume opens with *Orientation*, presents the five research papers as a bound sequence, and closes with the *Apparatus*. *Foundations* sets out the three general results both machines rest on. *Paper One* is the Hyperion breeder; *Paper Two* the Aegis / MetroVolt generator; *Papers Three, Four and Five* are the enabling science — high-field REBCO magnets and tape, direct energy conversion, and the AI / ML / quantum control stack. A *Digital Twin & 3-D Model* part follows, then the *Environmental* profile. The *Economics* and levelized cost and the *Business Case* and diligence record appear in the internal edition only; the *Simulations* proof record and the Apparatus — patent portfolio, team, limitations, and sources — close both editions.

THE FLEET AT A GLANCE

	HYPERION	AEGIS	METROVOLT
Role	Strategic-isotope foundry	Defense installation power	Campus power
Machine	**Spherical tokamak**	**Tandem mirror**	**Tandem mirror**
Fuel	Deuterium–tritium	Deuterium–helium-3	Deuterium–helium-3
Delivers	Tritium · ^{3}He · 14 MeV n	Resilient installation power	Firm campus power
Physics bar	**Fusion gain only**	Closure (gates named)	Closure + lunar ^{3}He
In the fleet	Breeds the fuel	Proves the generator	Commercial destination

HOW THE NUMBERS ARE MARKED

Every headline quantity carries an evidence class — DERIVED from first principles, RECOMPUTED from raw data, MEASURED in hardware, or a REQUIREMENT yet to be met. Financial figures carry a case label and are confined to the internal (confidential) edition. Values that moved after first publication are shown as withdrawn or restated rather than quietly changed. A capability you can evaluate is one whose limits are on the page.

ABSTRACT

Operating the Consumable Centrepost of a Compact Spherical-Tokamak Breeder: Demountable-Cartridge Swap Logistics, Fleet RAMI, and Centrepost Radial-Budget Reconciliation

The Hyperion breeder is built around a *consumable* centrepost: a demountable high-temperature-superconductor column that is periodically swapped rather than designed to survive the plant lifetime. That choice converts a hard material-lifetime problem into an operations problem whose soundness hinges on three coupled questions — how long a swap takes, how often it is required, and whether the column fits its radial envelope. We answer all three quantitatively and reconcile them into a single constrained program. First, the demountable-cartridge swap has a serial critical path of 21.5 days, of which cold-mass thermal cycling is 8.5 days ($40\,\%$) and the single dominant term. Second, we cast plant availability as an alternating-renewal process in which the operate phase ends when the centrepost fast-neutron fluence reaches its tolerance limit; the closed-form availability $A = \mathrm{CF}_0/(1 + \mathrm{CF}_0\, t_{\mathrm{swap}}/T_{\mathrm{life}})$ reproduces the frozen register anchors to within ≤ 0.5 percentage point, giving 0.582–0.590 at the design point and 0.638–0.648 at the mid-current point — a ≈5.7-point gain that identifies mid-current operation as the primary availability lever, with a further $+0.8$–1.0 point from merging the swap with pre-scheduled maintenance. We prove that a fractional gain in life and a fractional reduction in outage carry *equal and opposite* elasticity on availability, so the architecture's leverage lies where the achievable fractional change is largest: extending life from 0.21 to 0.46 full-power-years ($+119\,\%$) dominates the at-most $-40\,\%$ reachable from attacking the thermal term. Third, we establish *why* the swap governs: the lifetime synthesis shows the centrepost is *neutron-lifetime bound*, not stress-bound (181 MPa against a $6\times$ margin) and not quench-bound (multi-second protection), so the mid-current lever acts on the one limit that sets the cadence. Finally we reconcile the inboard radial build — a 30 cm neutron shield plus winding sums to 0.74 m against the $R_0 - a = 0.72$ m envelope, a ≈2 cm overrun bounded to a shield/winding re-optimization while the structural and quench budgets already pass. All results are frozen outputs of a verified reduced-order and GPU-accelerated Monte-Carlo campaign. The outcome is a quantified, honest operations basis for the consumable-centrepost architecture and a single, well-posed geometry item to close.

Open-access deposit (code & data, CC BY 4.0): DOI 10.5281/zenodo.22645931 · Zenodo community *kronos_fusion_energy*. Explore it live: interactive 3-D model · physics validator.

Keywords: demountable centrepost · RAMI · plant availability · renewal theory · swap logistics · radial build · consumable magnet · spherical-tokamak breeder

CONTENTS

Table of Contents

NOMENCLATURE

Symbols, units, and the names of things

Q	plasma (fusion) gain, P_{fus}/P_{aux}
Q_E	engineering gain, net electric out / recirculating in
H_{98}	confinement enhancement over the IPB98(y,2) scaling
Z_{eff}	effective ion charge
c_{ee}	electron–electron bremsstrahlung leading coefficient, 2.120022 (exact)
τ_E	energy confinement time
I_p	plasma current
R_0, a	major radius, minor radius
κ, δ	elongation, triangularity
β_N	normalized plasma beta (Troyon-normalized)
TBR	tritium breeding ratio
DEC	direct energy conversion
CF	plant capacity factor (availability)
FOAK / NOAK / BOAK	first / n^{th} / best of a kind
Hyperion	the ST breeder (internal: Mode D2)
Aegis	the generator, defense/installation housing (internal: Mode M)
MetroVolt	the generator, data-center housing (Mode M)

§ 1

Introduction

THE CONSUMABLE-CENTREPOST ARCHITECTURE

The compact spherical tokamak (ST) buys high fusion power density in a small volume by pushing the toroidal field as high as the inboard geometry will allow, which places the most heavily irradiated and most space-constrained magnet of the whole machine — the centrepost — directly against the plasma with almost no room for shielding [1,2,3]. In a conventional design the centrepost would have to survive the plant lifetime under a fast-neutron fluence that no present high-temperature superconductor (HTS) can tolerate. The Hyperion breeder makes the opposite architectural choice: the central column is a *demountable* rare-earth barium copper oxide (REBCO) cartridge that is replaced on a schedule, trading a hard material-lifetime problem for an operations problem [5,6]. The breeder's design point carries a centrepost peak field of 16.84 T at major radius $R_0 = 1.20$ m, aspect ratio $A = 2.5$ (minor radius $a = R_0/A = 0.48$ m), elongation $\kappa = 2.0$, negative triangularity $\delta = -0.30$, and delivers $Q = 3.076$, $P_{\text{fus}} = 85.04$ MW at plasma current $I_p = 9.66$ MA (Table 1). Its inboard radial envelope is therefore $R_0 - a = 0.72$ m — a budget that must simultaneously house the winding, its structure, and enough shield to buy a useful swap interval.

The operations problem this creates is the subject of the present paper. Three questions decide whether the consumable-centrepost architecture is sound:

[(i)] *How long is a swap?* The outage sets the denominator of plant availability.
[(ii)] *How often is a swap needed?* The cadence is set by whichever physical limit binds the column's life — and only if that limit is the neutron dose does the operations story we tell hold together.
[(iii)] *Does the column fit?* The winding-plus-shield stack must live inside $R_0 - a$, and the shield thickness is itself the knob that sets the life in (ii). enumerate
These three are not independent: the shield that lengthens the life in (ii) eats the radial budget in (iii), and the plasma current that raises the source strength shortens the life. We therefore treat them as one coupled program rather than three separate checks, and we answer each with frozen, reproduced numbers rather than a target.

PRIOR ART: DEMOUNTABLE MAGNETS, ST PILOT PLANTS, AND FUSION RAMI

Demountable toroidal-field magnets have a long pedigree in ST reactor studies precisely because they promise rapid in-vessel access and centrepost replacement [5,6,1]. The high-field-HTS route that makes a compact, replaceable column feasible rests on the maturation of REBCO coated conductors [9,10,11] and on demonstrations such as the 45.5 T all-superconducting user magnet [8]; the compact high-field tokamak programme more broadly is exemplified by SPARC and the ARC concept from which the demountable-magnet, replaceable-core idea descends [7,5]. What has been comparatively under-served is the *operations* layer that a consumable core forces to the foreground: reliability, availability, maintainability and inspectability (RAMI), the swap logistics, and the capacity-factor consequences of a scheduled magnet replacement. Fusion RAMI methodology is well developed for tokamak plant systems and for DEMO-class remote maintenance [24,25,22,23], but a consumable centrepost is a qualitatively different object: the single most availability-critical maintenance action is not a rare corrective outage but a *recurring, scheduled* one whose cadence is set by neutron damage physics [15,16,17,18]. This paper analyses that object directly.

The centrepost's physical limits and the neutronics that set its life have been established across the companion series: the coverage-versus-protection neutronics, coil integrity and fused quench detection of the consumable centrepost [doi:10.5281/zenodo.22645704; https://www.kronosfusionenergy.com/publications/centrepost-and-magnet-integrity.html]; the fast-fluence, dpa and shielding that set the cartridge-replacement cadence [doi:10.5281/zenodo.22645708; https://www.kronosfusionenergy.com/publications/centrepost-fluence-and-shielding.html]; the first-principles radiation tolerance of the centrepost REBCO itself [doi:10.5281/zenodo.22645923; https://www.kronosfusionenergy.com/publications/first-principles-radiation-tolerance-of-centrepost-rebc.html]; and the REBCO high-field conductor and winding basis [doi:10.5281/zenodo.22645697; https://www.kronosfusionenergy.com/publications/magnets.html]. The lifetime-constrained operating-window synthesis [doi:10.5281/zenodo.22645799; https://www.kronosfusionenergy.com/publications/admissible-operating-window-synthesis.html] fixes the admissible plasma-current range that the mid-current lever exploits, the cold-mass thermal budget that governs the dominant swap term is set in the cryogenics analysis [doi:10.5281/zenodo.22645840; https://www.kronosfusionenergy.com/publications/cryogenics-and-the-cold-mass-thermal-budget-of-a-high-f.html], the per-column remaining-useful-life prognostics that schedule the swap are developed separately [doi:10.5281/zenodo.22645788; https://www.kronosfusionenergy.com/publications/centrepost-prognostics-and-rul-control.html], and the propagation of the swap cadence to a four-unit fleet capacity factor is treated by time-domain Monte-Carlo in the fleet-availability study [doi:10.5281/zenodo.22645951; https://www.kronosfusionenergy.com/publications/fleet-availability-under-consumable-centre-post-swap-cad.html]. The present paper is the single-unit operations spine that ties those results together.

CONTRIBUTION

We make four contributions. (1) We give the swap critical path a defensible decomposition and name its dominant term. (2) We cast plant availability as an alternating-renewal process whose closed form reproduces the frozen register anchors to $\leq \mathbf{0.5}$ point, and we prove the life–outage elasticity identity that explains why mid-current operation, and not thermal-term surgery, is the architecture's primary availability lever. (3) We establish that the swap governs availability because the column is neutron-lifetime bound — demonstrated against a structurally and thermally sound magnet — and we tie the mid-current lever to the admissible operating-current window. (4) We reconcile the inboard radial build to a bounded ≈2 cm overrun and pose the closure as a single constrained-optimization item. Throughout, every number is a frozen output of the Kronos de-risking register reproduced in a verified reduced-order and GPU-accelerated Monte-Carlo campaign (§3).

§ 2

Governing equations and the formal problem

DESIGN ANCHORS AND GEOMETRY

Table 1 collects the frozen anchors that govern the analysis. The inboard radial envelope $R_0 - a = 0.72$ m and the centrepost peak field 16.84 T are the geometry constraints; I_p, P_{fus} and Q fix the neutron source strength and hence the damage rate.

QUANTITY	SYMBOL	VALUE
major radius	R_0	1.20 m
aspect ratio	A	2.5
minor radius	$a = R_0/A$	0.48 m
inboard envelope	$R_0 - a$	0.72 m
elongation	κ	2.0
triangularity	δ	-0.30
on-axis field	B_0	8 T
centrepost peak field	B_{cp}	16.84 T
plasma current	I_p	9.66 MA
fusion power	P_{fus}	85.04 MW
fusion gain	Q	3.076
centrepost damage rate	D	18.85 dpa fpy^{-1}
first-wall load	Γ_{w}	1.885 MW m^{-2}

Frozen design anchors and derived geometry for the Hyperion breeder centrepost (Tier-2 canon; register serials BR-L1-A1, BR-L1-A7, BR-L1-A13).

FLUENCE-LIMITED CENTREPOST LIFE

The centrepost life is set by radiation damage to the REBCO conductor, not by mechanical or thermal margin (§4.3). Let φ_{cp} be the fast-neutron flux ($E > 0.1$ MeV) at the conductor monitor plane and Φ_c the fluence tolerance limit at which the critical current has degraded to its acceptance floor. The accumulated fluence after τ full-power-years is $\Phi(\tau) = \varphi_{\text{cp}}\,\tau$, so the life is

$$T_{\text{life}} \;=\; \frac{\Phi_c}{\varphi_{\text{cp}}(t_s, I_p)},$$

where the flux depends on the inboard shield thickness t_s (which attenuates the source) and on I_p (which sets the source strength). The damage bookkeeping is the standard Norgett–Robinson–Torrens (NRT) displacement model [15], in which the displacement rate folds the flux against a displacement cross-section,

$$R_{\text{dpa}} \;=\; \int_{E_{\min}}^{E_{\max}} \varphi(E)\,\sigma_{\text{disp}}(E)\,\mathrm{d}E, \qquad \nu_{\text{NRT}}(T_{\text{dam}}) \;=\; \frac{0.8\,T_{\text{dam}}}{2E_d},$$

with $T_{\rm dam}$ the damage energy and E_d the displacement threshold; the athermal-recombination-corrected ("arc-dpa") model of [16] refines $\nu_{\rm NRT}$ downward at high recoil energy and is used as a cross-check. At the design shield the code returns $D = 18.85\,\mathrm{dpa\,fpy}^{-1}$ (BR-L1-A13), and the fast-fluence proxy sets $T_{\rm life} = 0.21\,\mathrm{fpy}$ at the design point. Equations 1–2 make the two operating levers explicit: raising t_s lowers $\varphi_{\rm cp}$ (Fig. 4) and lowering I_p lowers the source strength (Fig. 5); both lengthen $T_{\rm life}$.

THE ALTERNATING-RENEWAL AVAILABILITY MODEL

Because the centrepost is swapped on a fluence schedule, the plant executes an *alternating renewal process* [26,27,28]: an operate phase of calendar length $t_{\rm op}$, followed by a swap outage of length $t_{\rm swap}$, repeated. During the operate phase the machine runs at a baseline capacity factor CF_0 that folds in every *non*-swap outage (planned maintenance, forced outages, fuelling, ramps); the phase ends when the accumulated fast fluence reaches Φ_c, i.e. when it has delivered exactly $T_{\rm life}$ full-power-years. The calendar length of the operate phase is therefore

$$t_{\rm op} \;=\; \frac{T_{\rm life}}{\mathrm{CF}_0},$$

and the renewal-cycle length is $t_{\rm cyc} = t_{\rm op} + t_{\rm swap}$. By the renewal-reward theorem the long-run availability (the achieved capacity factor) is the ratio of delivered full-power-years to elapsed calendar time per cycle,

$$A \;=\; \frac{T_{\rm life}}{t_{\rm op}+t_{\rm swap}} \;=\; \frac{T_{\rm life}}{\dfrac{T_{\rm life}}{\mathrm{CF}_0}+t_{\rm swap}} \;=\; \frac{\mathrm{CF}_0}{1+\mathrm{CF}_0\,\dfrac{t_{\rm swap}}{T_{\rm life}}}\,.$$

Equation 4 is the central result of the operations analysis. It has the correct limits: $A \to \mathrm{CF}_0$ as $T_{\rm life}\to\infty$ (the swap-free machine recovers the baseline capacity factor), and $A \to \mathrm{CF}_0\,T_{\rm life}/(\mathrm{CF}_0\,t_{\rm swap}) = T_{\rm life}/t_{\rm swap}$ as $T_{\rm life}\to 0$ (a machine that must be swapped continuously delivers only the duty ratio of an operate sliver to a full outage). The entire swap penalty is carried by a single dimensionless group,

$$\eta \;\equiv\; \frac{\mathrm{CF}_0\,t_{\rm swap}}{T_{\rm life}}, \qquad \frac{A}{\mathrm{CF}_0} \;=\; \frac{1}{1+\eta},$$

so that A/CF_0 is the *availability retention* against the swap-free baseline. The number of swaps over a plant life L is the renewal count

$$N_{\rm swap} \;=\; \left\lfloor \frac{L}{t_{\rm cyc}} \right\rfloor \;=\; \left\lfloor \frac{A\,L}{T_{\rm life}} \right\rfloor.$$

Merging the swap with pre-scheduled maintenance of overlap $\Delta_{\rm ov}$ (work that would occur anyway and can be hidden behind the swap outage) replaces $t_{\rm swap}$ by an effective marginal outage $t^{\rm eff}_{\rm swap} = t_{\rm swap} - \Delta_{\rm ov}$ in 4.

LEVERAGE: LIFE VERSUS OUTAGE

Because A in 4 depends on $T_{\rm life}$ and $t_{\rm swap}$ only through their ratio, the two control variables have equal-and-opposite logarithmic sensitivity. Writing the elasticities,

$$\frac{\partial \ln A}{\partial \ln T_{\rm life}} \;=\; \frac{\eta}{1+\eta} \;=\; -\,\frac{\partial \ln A}{\partial \ln t_{\rm swap}}\,,$$

so a 1% increase in centrepost life and a 1% decrease in outage duration are *exactly* equally valuable. The architecture's leverage therefore lies not in which variable is more potent per unit — they are identical — but in which variable admits the larger *achievable fractional change*. Moving to the mid-current point extends life from 0.21 to $0.46\,\mathrm{fpy}$, a $+119\,\%$ change, whereas the entire thermal term is $40\,\%$ of the outage, so even its complete elimination is a $-40\,\%$ change in $t_{\rm swap}$. Mid-current operation is thus the larger lever by construction, and the two combine multiplicatively through η.

THE RADIAL-BUDGET CONSTRAINT AND THE COUPLED PROGRAM

The inboard build must fit the envelope. With radial thicknesses $t_{\rm wind}$ (winding plus structure), t_s (shield) and $t_{\rm fw}$ (first wall plus gap), the geometric constraint is

$$t_{\rm wind}(I_p) + t_s + t_{\rm fw} \;\le\; R_0 - a \;=\; 0.72\ \mathrm{m}.$$

Combining 1, 4 and 8 yields the operations optimum as a single constrained program: choose the shield thickness and plasma current that maximise availability subject to the radial budget and the physics window,

$$\max_{t_s,\, I_p} \; A\big(T_{\text{life}}(t_s, I_p),\, t_{\text{swap}}\big) \quad \text{s.t.} \quad (???),\;\; I_p \in [\,I_p^{\min},\, I_p^{\max}\,],\;\; q_{95} \geq q_{95}^{\min},$$

where $[\,I_p^{\min}, I_p^{\max}\,]$ is the admissible operating-current window of §4.5. The tension in 9 is direct: increasing t_s lengthens T_{life} and raises A but consumes the radial budget in 8; the frozen design sits at the point where a **30** cm shield gives $T_{\text{life}} = \mathbf{0.21}$ **fpy** but the stack overruns 8 by ≈2 cm (§4.8). This is the sole active constraint left to close.

§ 3

Computational methodology: the NVIDIA GPU HPC campaign

Every number in this paper is a frozen output of the Kronos physics de-risking campaign, executed on the NVIDIA GPU HPC fleet (A100 / H100 / A10 partitions) with a reduced-order verification tier that runs on commodity nodes. This section names the codes actually run for the underlying serials, the discretization and solver for each, and the verification that makes the results reproducible. No cost or spend figures are reported anywhere; the compute is described only by code, problem scale and accelerator class.

CODES AND THEIR ROLES

Table 2 lists the solvers behind each frozen result. Three engines carry the analysis: (i) OpenMC [13] with ENDF/B-VIII.0 nuclear data [14] for the fast-fluence and displacement-damage maps that set $T_{\rm life}$; (ii) the KRONOS reduced-order toolkit for the 0-D power/particle balance and the operating-window synthesis that fixes $[I_p^{\min}, I_p^{\max}]$; and (iii) the RAMI renewal solver implementing 4–6 in closed form and as a time-domain Monte-Carlo. Structural finite-element and quench sub-models establish that the column is neither stress- nor quench-bound.

RESULT	SERIAL	CODE / METHOD	TIER	
**swap critical path **	availability	BR-SX-18	RAMI renewal (closed form + MC)	LOCAL
centrepost lifetime synthesis	BR-SX-16	neutronics + FE + quench synthesis	GPU / LOCAL	
**fast fluence **	dpa vs shield	BR-L1-A13b	OpenMC (ENDF/B-VIII.0)	GPU
displacement damage rate	BR-L1-A13	OpenMC damage-energy (NRT/arc-dpa)	GPU	
3-D neutron transport balance	BR-L1-A5	OpenMC, 1.2×10^8 histories	GPU	
admissible current window	KX-L1-A21	reduced-order window synthesis (61 q_{95} pts)	LOCAL	
radial-budget reconciliation	BR-SXD-06	CSG radial build + constraint check	LOCAL	

Codes run for the frozen results, their role, and accelerator class. LOCAL = commodity reduced-order tier; GPU = NVIDIA A100/H100/A10 fleet.

NEUTRON TRANSPORT AND DISPLACEMENT DAMAGE

The fast-fluence and damage maps that fix $T_{\rm life}(t_s)$ come from OpenMC, a continuous-energy Monte-Carlo particle-transport code [13], run against ENDF/B-VIII.0 evaluated nuclear data [14]. The full-machine 3-D balance (BR-L1-A5) is tallied over 1.2×10^8 source histories, giving a first-wall fast flux of 7.0×10^{14} n cm^{-2} s^{-1}, a global leakage of 0.121 and a nuclear heating of 74.6 MW; the shield trade (BR-L1-A13b) uses a 1-D infinite-cylinder constructive-solid-geometry (CSG) model of the inboard build — concentric z-cylinders about the machine axis with a reflective axial boundary — to isolate the shield-thickness dependence cleanly. The trade knob is $t_s \in \{0, 15, 30, 45\}$ cm of tungsten-carbide mantle (BR-L1-A13b sets $t_s = 45 - \mathrm{ib\_mantle}$). Displacement damage is scored with the NRT damage-energy tally of 2 and cross-checked against the arc-dpa correction of [16]. Monte-Carlo statistical error scales as $N^{-1/2}$ in the history count N; tallies are batched with the standard error propagated to the fluence and damage estimates. The absolute "life" uses fast-fluence damage-limit proxies (10^{22}–10^{23} n m^{-2}, $E > 0.1$ MeV) rather than a full REBCO critical-current degradation curve, and the centrepost is modelled as a homogenized Cu + SS bundle (a REBCO-centrepost proxy) rather than at tape level — both honest simplifications carried forward from the register.

REDUCED-ORDER OPERATING-WINDOW SYNTHESIS

The admissible current window (KX-L1-A21) is computed with the KRONOS reduced-order toolkit's `evaluate_breeder` 0-D power/particle-balance solver, which fixes the point self-consistently to the frozen anchors ($Q = 3.076$, $P_{\text{fus}} = 85.04$ MW, $I_p = 9.66$ MA) by Newton iteration and then scans q_{95} over 61 points in $[2.7, 3.3]$. Each point returns (I_p, P_{fus}, D); the window is the feasible set $\mathcal{W} = \{p : g_k(p) \leq 0\ \forall k\}$ intersecting the MHD-edge floor ($q_{95} \geq q_{95}^{\text{min}}$) below and the centrepost-fluence ceiling ($D \leq D_{\text{DP}} = 18.85$ dpa fpy^{-1}) above. The tritium-startup floor is checked and found non-binding (minimum $T = 3.17$ kg yr^{-1} against a 1.87 kg yr^{-1} duty floor).

THE RAMI RENEWAL SOLVER

The availability model of §2.3 is evaluated two ways for mutual verification. The closed form 4 is evaluated directly at the frozen $(T_{\text{life}}, t_{\text{swap}}, \text{CF}_0)$. Independently, a time-domain Monte-Carlo advances the fluence accumulation as a sawtooth — integrating CF_0 over calendar time, resetting at each swap, and drawing the outage from the frozen critical-path distribution — to produce the 30-year cadence trace of Fig. 6 and the swap count 6. The two agree to within the Monte-Carlo error, and both reproduce the frozen register availability anchors to ≤ 0.5 percentage point (Table 3).

STRUCTURAL AND QUENCH SUB-BUDGETS

The lifetime synthesis (BR-SX-16) closes the “which limit binds” question with two supporting sub-models. A structural finite-element evaluation of the centrepost under the 16.84 T Lorentz load returns a peak von Mises stress of 181 MPa against a $6\times$ margin to the conductor/structure allowable; the quench-protection model returns a multi-second adiabatic hot-spot timescale. Both are comfortably non-binding, isolating the neutron dose as the sole life-limiter (§4.3). A reviewer audit confirmed that the structural finite-element “PASS” is a *structural-only* statement and does not override the neutron-lifetime bound; the two are distinct and both are reported.

VERIFICATION AND REPRODUCIBILITY

The reduced-order engine reproduces $19/19$ frozen anchors (KX-L1-A6, KX-L1-A10), the neutronics is cross-checked against the frozen anchors and, where available, an independent GPU-fleet run and alternate nuclear-data/analytic estimates, and the availability closed form is cross-verified against the time-domain Monte-Carlo. Seeds, code versions and node classes are recorded per serial in the de-risking register (§7).

§ 4

Results

THE SWAP CRITICAL PATH

A cartridge swap has a serial critical path of 21.5 days (BR-SX-18; Fig. 1). The single largest term is cold-mass thermal cycling — warming the demountable joint and cold mass enough to make the mechanical break, then re-cooling to 4.5 K — at 8.5 days, or 40 % of the outage. The remaining 13.0 days cover the mechanical break-and-remake of the demountable joint, cartridge extraction and insertion, and re-qualification (Fig. 9b). The decomposition is operationally useful because it names the term to attack: nearly half the outage is thermal, so any reduction in the cold-mass thermal cycle — staged pre-cooling, a warmer demountable joint, or parallelised cartridge conditioning — acts directly on the dominant contributor. The thermal term is set by the cold-mass heat capacity and the refrigeration ramp analysed in the cryogenics companion [doi:10.5281/zenodo.22645840; https://www.kronosfusionenergy.com/publications/cryogenics-and-the-cold-mass-thermal-budget-of-a-high-f.html].

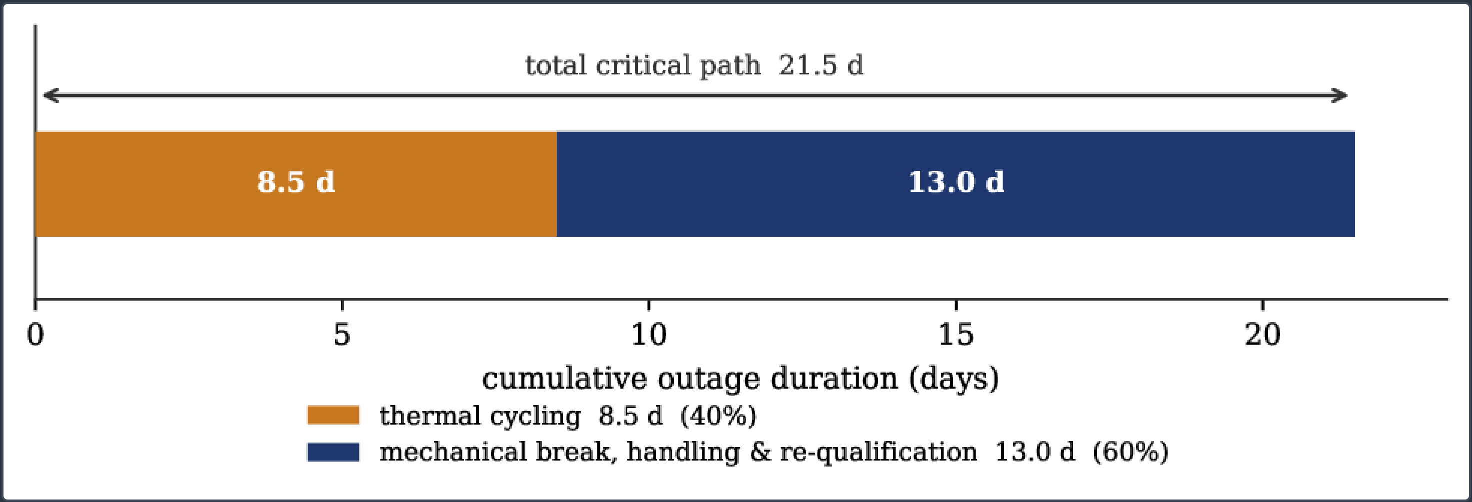

The 21.5-day cartridge-swap critical path (BR-SX-18). Cold-mass thermal cycling (8.5 d, 40 %) is the dominant single term; the mechanical break-remake, cartridge handling and re-qualification make up the remaining 13.0 d.

AVAILABILITY AND THE MID-CURRENT LEVER

Inserting the frozen $(T_{\text{life}}, t_{\text{swap}}, \text{CF}_0)$ into the renewal availability 4 reproduces the register anchors closely (Table 3). At the design point ($T_{\text{life}} = 0.21$ fpy) the unmerged model returns $A = 0.578$ and the merged-cadence model ($\Delta_{\text{ov}} \approx 4$ d) returns $A = 0.596$, bracketing the frozen range 0.582–0.590; at the mid-current point ($T_{\text{life}} = 0.46$ fpy) the model returns $A = 0.634$ unmerged and 0.644 merged, inside the frozen range 0.638–0.648. Figure 2 plots the full $A(T_{\text{life}})$ curve with both anchors, and Figure 3 shows the design-versus-mid-current step against the $\text{CF}_0 = 0.69$ baseline. The ≈5.7-point gain from mid-current operation is the single largest availability lever in the architecture. Its origin is exactly 7: mid-current extends the neutron life by +119 %, and through the availability retention $A/\text{CF}_0 = 1/(1+\eta)$ this shrinks the swap-penalty group η from 0.194 to 0.088, lifting retention from 0.838 to 0.919. Merging the swap with pre-scheduled maintenance adds a further +0.8–1.0 point at either operating point.

QUANTITY	DESIGN POINT	MID-CURRENT POINT
centrepost life T_{life}	0.21 fpy	0.46 fpy
swap-penalty group η 5	0.194	0.088
availability retention A/CF_0	0.838	0.919
model A (unmerged)	0.578	0.634
model A (merged, −4 d)	0.596	0.644

table continued

frozen register range	0.582–0.590	0.638–0.648
swaps over 30 yr 6 (model)	71	38
frozen register (mid-current)	—	≈ 39

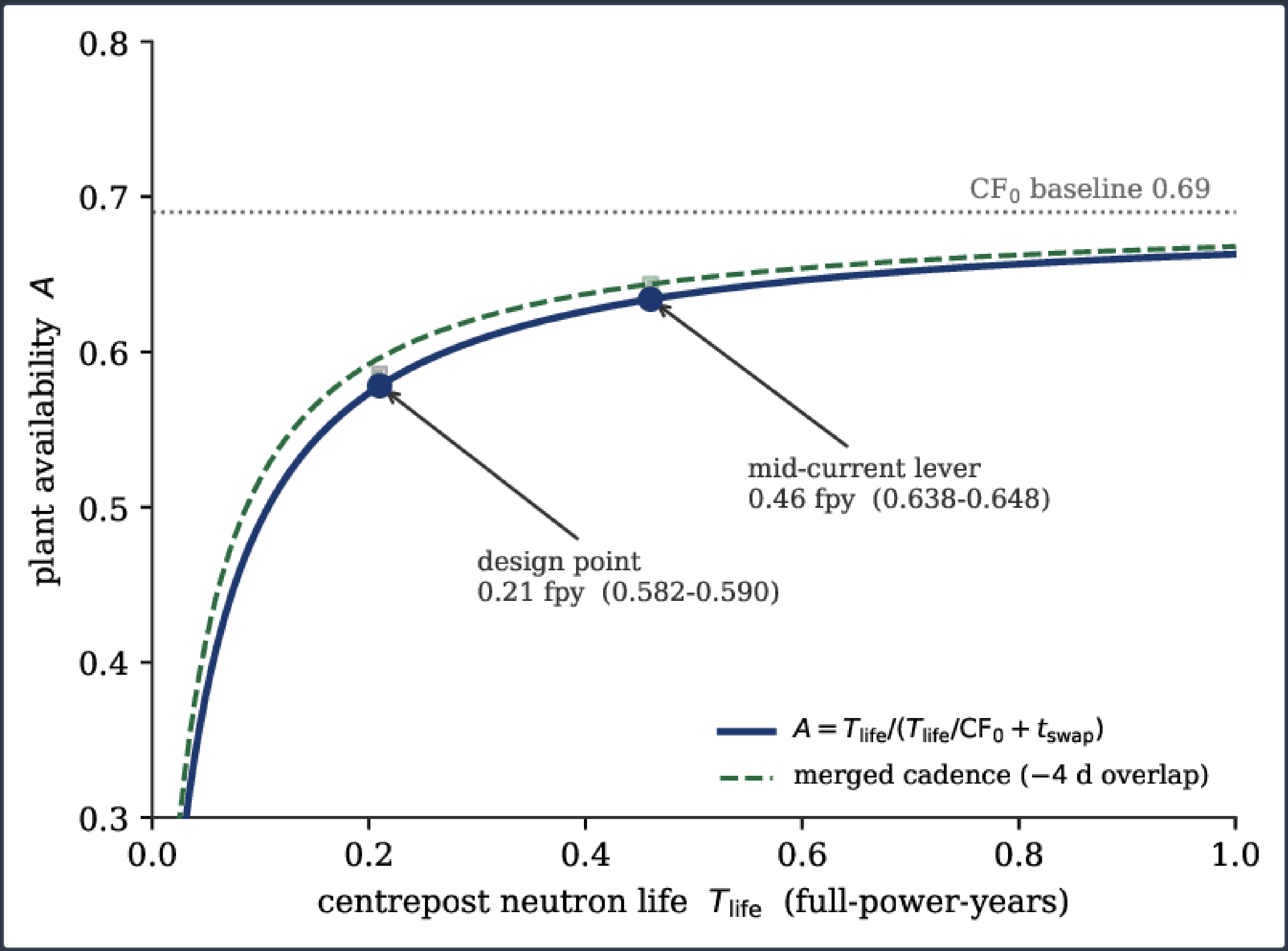

Renewal-model availability $A(T_{\text{life}}) = \text{CF}_0/(1 + \text{CF}_0\, t_{\text{swap}}/T_{\text{life}})$ 4 with $\text{CF}_0 = 0.69$, $t_{\text{swap}} = 21.5$ d (solid) and merged cadence (dashed). Shaded bands are the frozen register anchors at the design (0.21 fpy) and mid-current (0.46 fpy) lives; the model passes through both. The curve asymptotes to the CF_0 baseline only as $T_{\text{life}} \to \infty$.

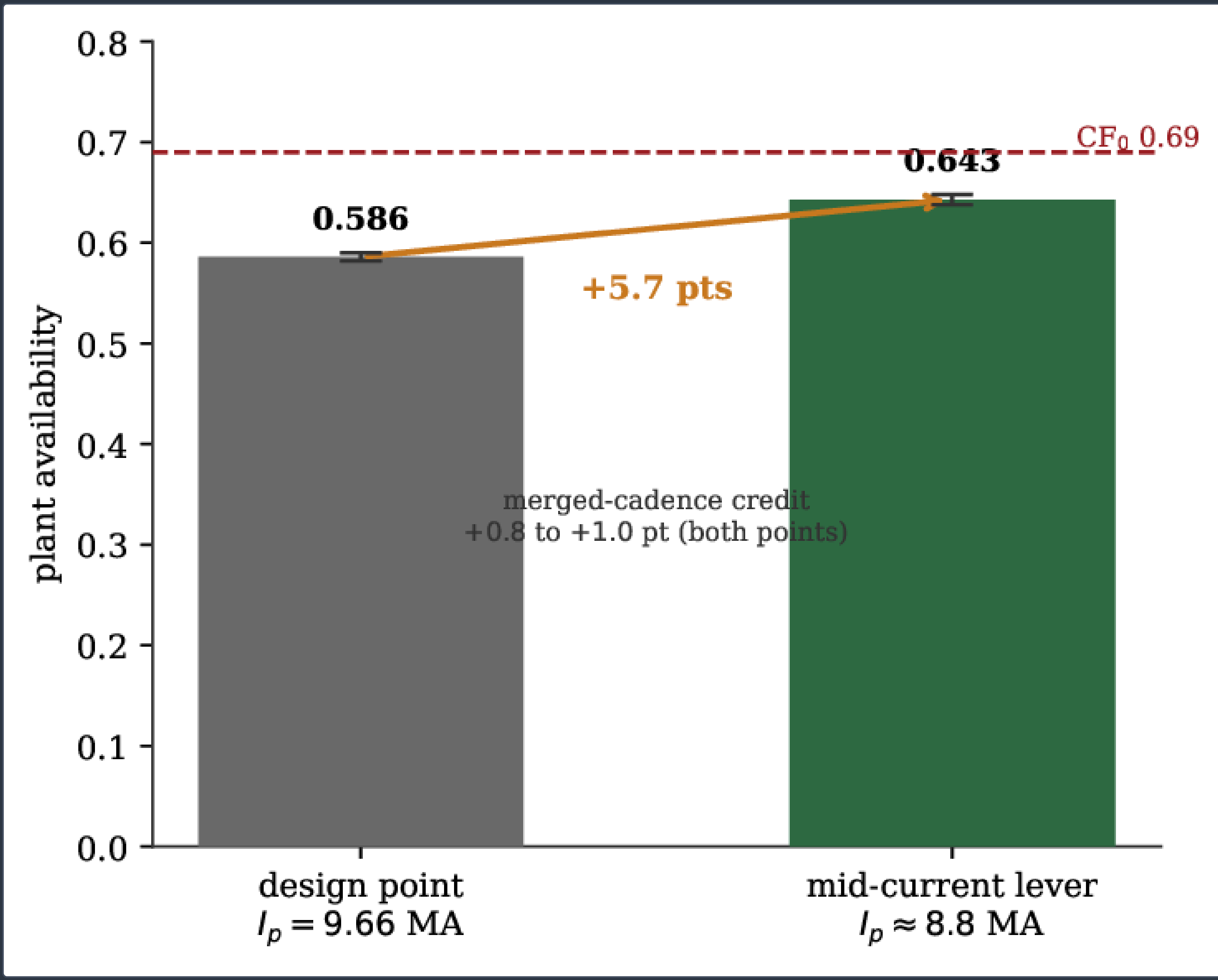

Plant availability at the design point (0.582–0.590) and the mid-current lever (0.638–0.648); error bars span the frozen ranges. The ≈5.7-point step is the architecture's primary availability lever. Both points sit below the swap-free baseline $\mathrm{CF}_0 = 0.69$ (dashed), which is the honest headline: the swap cadence costs availability, and mid-current is the recovery lever.

WHY THE SWAP GOVERNS: THE CENTREPOST IS NEUTRON-LIFETIME BOUND

The operations case rests on knowing which physical limit sets the swap interval, and the lifetime synthesis (BR-SX-16) settles it: the centrepost is *neutron-lifetime bound*, not stress-bound and not quench-bound. Structurally the column carries 181 MPa against a 6× margin, and its quench-protection timescale is multi-second, so neither is the binding constraint; the limit is the fast-neutron dose to the REBCO through 1, giving $T_{\mathrm{life}} = 0.21$ fpy at the design point and 0.46 fpy at mid-current. This is precisely why mid-current operation is the availability lever: through 7 it acts on the one variable that actually sets the cadence. The coil-integrity and fused quench-detection basis for this conclusion is developed in the consumable-centrepost companion [doi:10.5281/zenodo.22645704; https://www.kronosfusionenergy.com/publications/centrepost-and-magnet-integrity.html], and the underlying REBCO radiation tolerance in the first-principles study [doi:10.5281/zenodo.22645923; https://www.kronosfusionenergy.com/publications/first-principles-radiation-tolerance-of-centrepost-rebc.html].

THE CENTREPOST LIFE–SHIELD TRADE

Equation 1 is dominated by the shield attenuation. The OpenMC shield trade (BR-L1-A13b) shows that a tungsten-carbide mantle from 0 to 45 cm cuts the centrepost fast fluence from 2.9×10^{25} to 1.7×10^{23} $\mathrm{n\,m^{-2}\,fpy^{-1}}$ — two orders of magnitude — lifting the life from 0.003 to 0.58 fpy (Fig. 4, Table 4). The design sits near 30 cm, giving $T_{\mathrm{life}} = 0.21$ fpy; a thicker shield would lengthen life further but at the cost of the radial budget 8 — exactly the tension in the coupled program 9. This trade is the subject of the centrepost life-limiter companion [doi:10.5281/zenodo.22645708; https://www.kronosfusionenergy.com/publications/centrepost-fluence-and-shielding.html].

WC SHIELD (CM)	FAST FLUENCE (N M^{-2} fpy^{-1})	LIFE (FPY)
0	2.9×10^{25}	0.003
15	$\sim 2.0 \times 10^{24}$	~ 0.05
30	$\sim 2.2 \times 10^{23}$	0.21 (design)
45	1.7×10^{23}	0.58

Centrepost life–shield trade from 1-D OpenMC (BR-L1-A13b). End anchors are frozen register values; interior points are the monotone trade the register reports. WC = tungsten carbide.

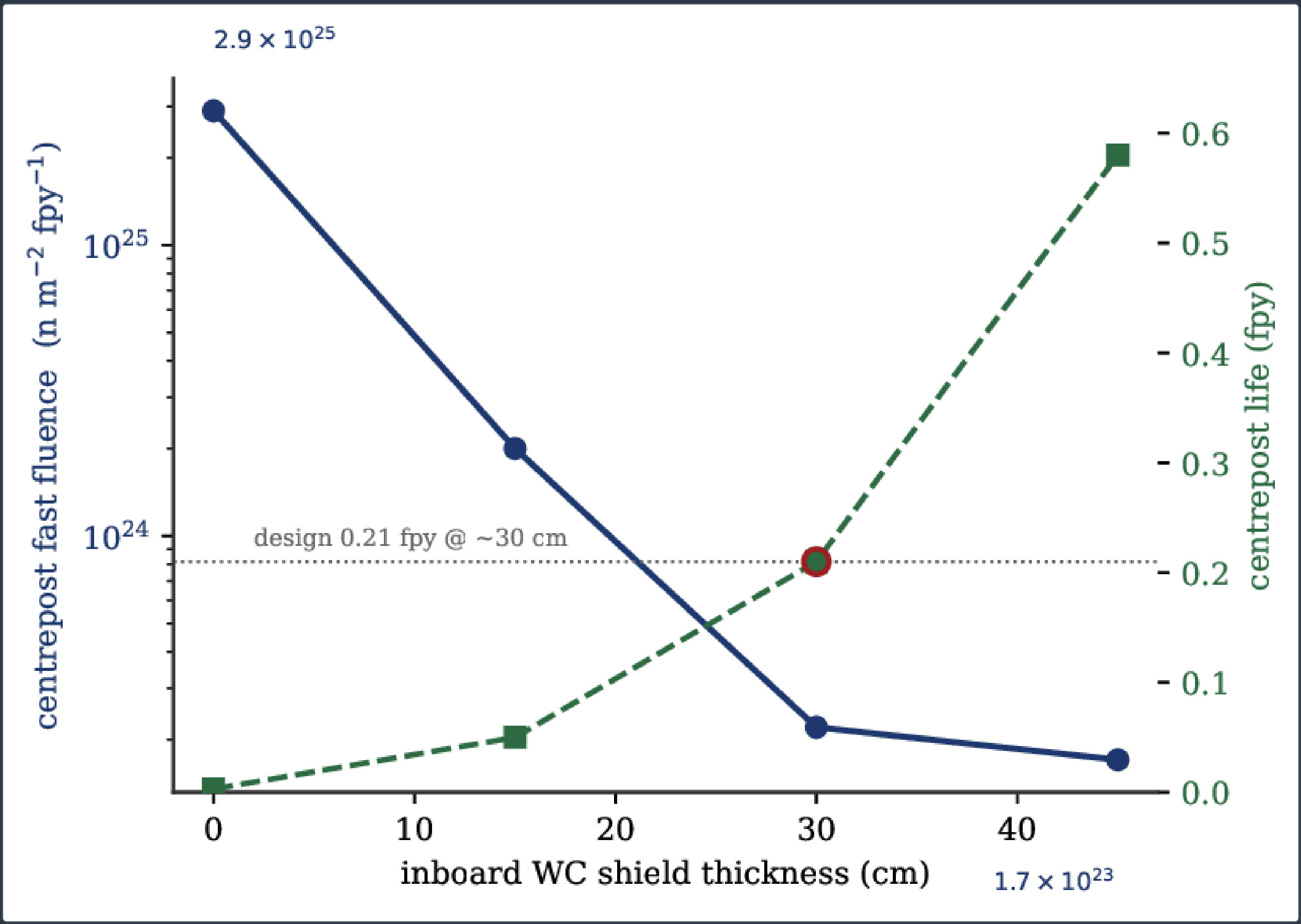

Centrepost fast fluence (left axis, log) and life (right axis) versus inboard WC shield thickness (BR-L1-A13b). The design point (red circle) sits near a 30 cm shield giving 0.21 fpy; the end anchors $2.9 \times 10^{25} \rightarrow 1.7 \times 10^{23}$ $\mathrm{n\,m^{-2}\,fpy^{-1}}$ and $0.003 \rightarrow 0.58$ fpy are frozen register values.

THE ADMISSIBLE OPERATING-CURRENT WINDOW

The mid-current lever is bounded by physics. The operating-window synthesis (KX-L1-A21) returns an admissible plasma-current window $I_p \in [8.779, 9.656]$ MA over $q_{95} \in [2.7, 3.3]$, floored below by the MHD q_{95} edge and ceilinged above by the centrepost damage rate $D \leq 18.85$ dpa fpy^{-1} (Fig. 5, Table 5). The design point sits at the ceiling ($I_p = 9.656$ MA, $D = 18.85$), and the mid-current lever moves down the window toward $I_p = 8.779$ MA ($D = 15.58$ dpa fpy^{-1}, $P_{\text{fus}} = 70.28$ MW), lowering the source strength in 1 and lengthening life. The tritium-startup floor does not bind (it would only bind near 41.5 MW), so the window is genuinely available to the operations plan. The full synthesis is the operating-window companion [doi:10.5281/zenodo.22645799; https://www.kronosfusionenergy.com/publications/admissible-operating-window-synthesis.html].

POINT	q_{95}	I_p (MA)	D (DPA fpy^{-1})
MHD-edge ceiling (max I_p)	2.70	10.729	23.28
design point	≈ 2.90	9.656	18.85
mid-current lever	3.30	8.779	15.58

Admissible operating-current window endpoints and design point (KX-L1-A21). The window is MHD-edge-limited below and centrepost-fluence-limited above.

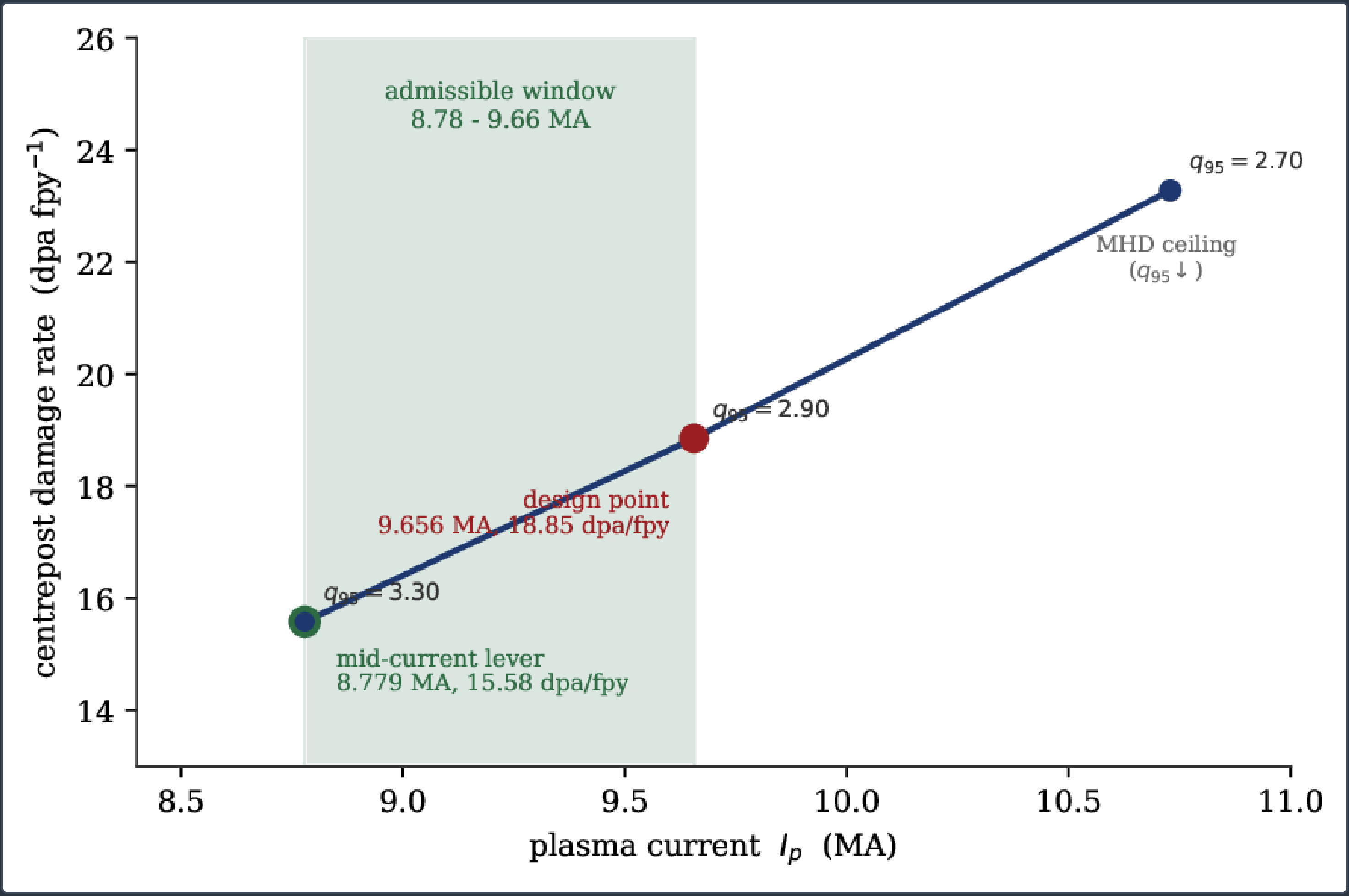

Admissible operating-current window (KX-L1-A21): centrepost damage rate versus I_p along the $q_{95} \in [2.7, 3.3]$ scan. The shaded band is the admissible window $I_p \in [8.779, 9.656]$ MA; the design point (red) sits at the fluence ceiling, and the mid-current lever (green) moves down-current to lengthen the neutron life.

SWAP CADENCE OVER THE PLANT LIFE

Figure 6 shows the time-domain Monte-Carlo fluence accumulation over a 30-year plant life: a sawtooth that resets at each swap. At the design life the plant executes many short cycles; at the mid-current life it executes ≈ 40 (model: 38; frozen register: ≈ 39 via 6), each cycle roughly twice as long. Fewer, longer cycles mean fewer 21.5-day outages per decade, which is the mechanism by which the life extension converts into the availability gain of §4.2. The per-column remaining-useful-life scheduling that triggers each reset is developed in the prognostics companion [doi:10.5281/zenodo.22645788; https://www.kronosfusionenergy.com/publications/centrepost-prognostics-and-rul-control.html].

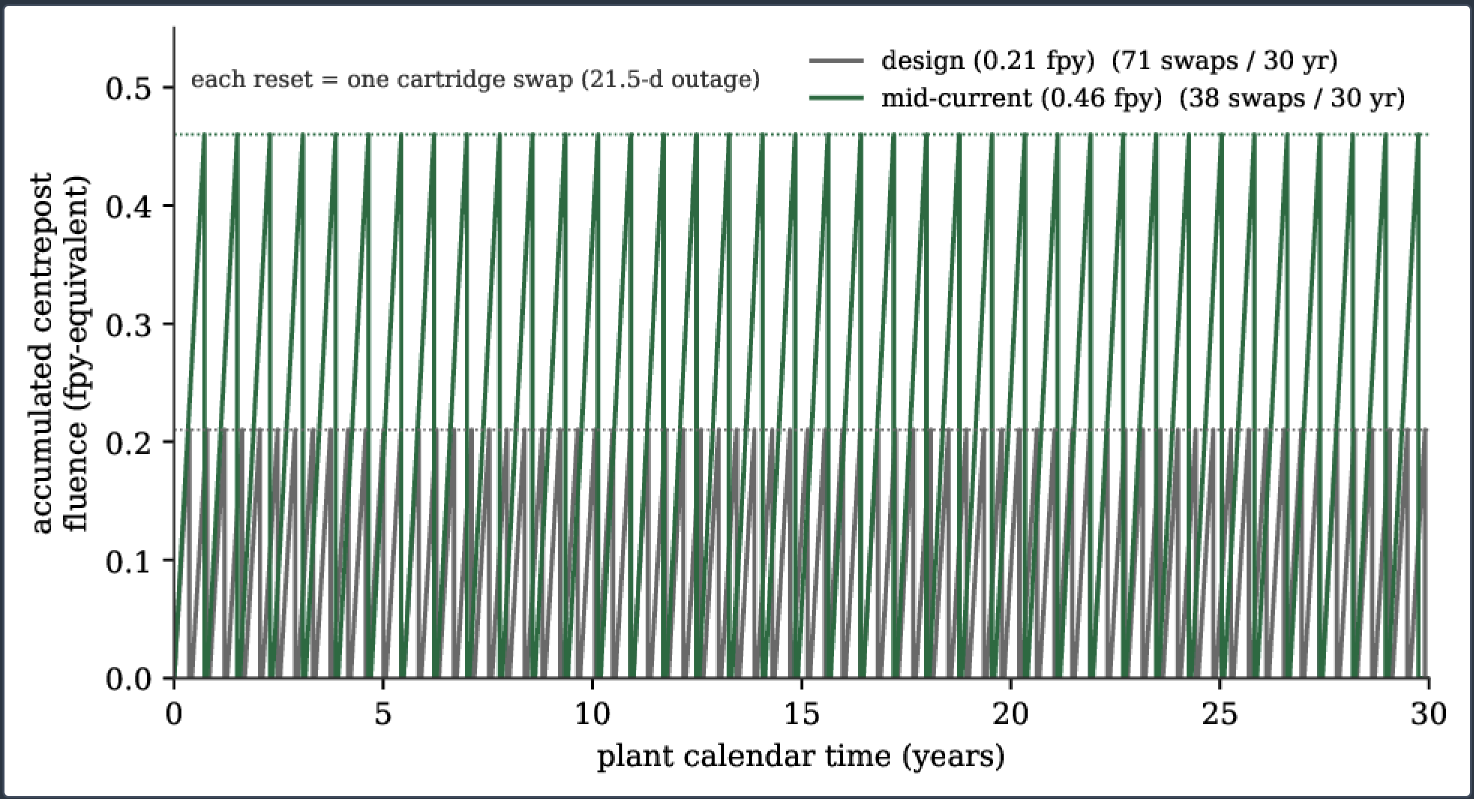

Time-domain fluence accumulation over the 30-year plant life at the design (0.21 fpy) and mid-current (0.46 fpy) lives. Each reset is a cartridge swap (a 21.5-day outage); the mid-current case executes ≈ 40 swaps versus far more at the design life, which is why the life extension buys availability.

SENSITIVITY TO OUTAGE DURATION

Figure 7 evaluates 4 as t_{swap} varies, at both lives. Consistent with the elasticity identity 7, the availability sensitivity to outage is real but its *reach* is limited by the 8.5-day thermal term: halving the thermal cycle (−4.25 d) or eliminating it entirely (−8.5 d) moves the mid-current availability by roughly +1 and +2 points respectively — worthwhile, but smaller than the ≈5.7-point mid-current lever. This is the quantitative basis for prioritising mid-current operation first and thermal-term reduction second.

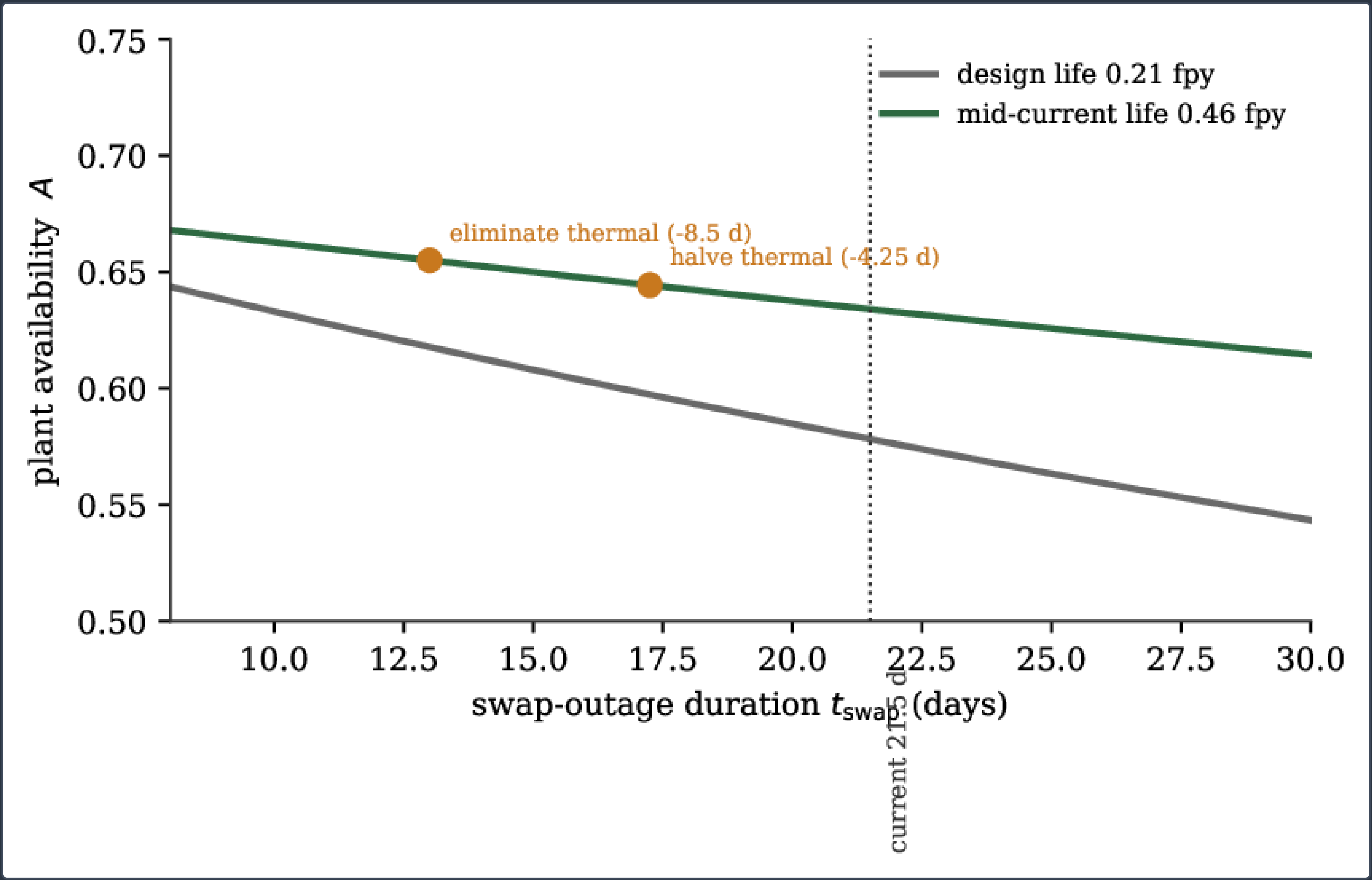

Availability versus swap-outage duration 4 at the design and mid-current lives. The current outage is 21.5 d; the amber markers show the mid-current availability if the 8.5-day thermal term is halved or eliminated. Outage reduction helps, but its reach is bounded by the thermal term.

THE RADIAL-BUDGET RECONCILIATION

The last question is geometric. Reconciling the inboard build (BR-SXD-06), the magnet winding plus a **30** cm neutron shield sums to **0.74** m against the $R_0 - a = 0.72$ m envelope of 8 — a ≈2 cm overrun (Fig. 8). The reconciliation is well-posed because everything around it already passes: the structural budget (**181** MPa, **6**× margin) and the quench budget are met at the **16.84** T operating field, so the overrun is a pure build-thickness reconciliation — to be closed by shield/winding re-optimization or a modest geometry relief in 9 — not a symptom of a structural or thermal shortfall. It is the single open geometry item in the centrepost operations case, and it is bounded at the centimetre scale.

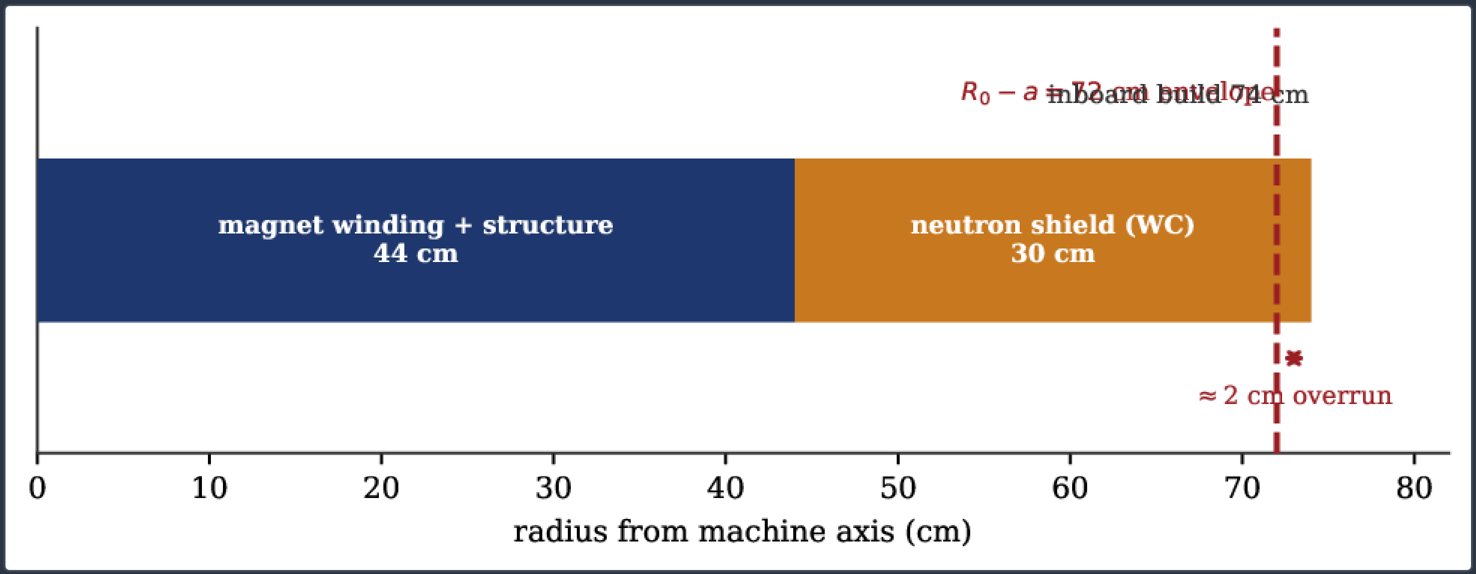

Inboard radial-budget reconciliation (BR-SXD-06). Winding-plus-structure and a **30** cm WC shield sum to ≈ **0.74** m against the $R_0 - a = 0.72$ m envelope (red dashed), a ≈2 cm overrun to be closed by shield/winding re-optimization. The structural and quench budgets already pass at **16.84** T.

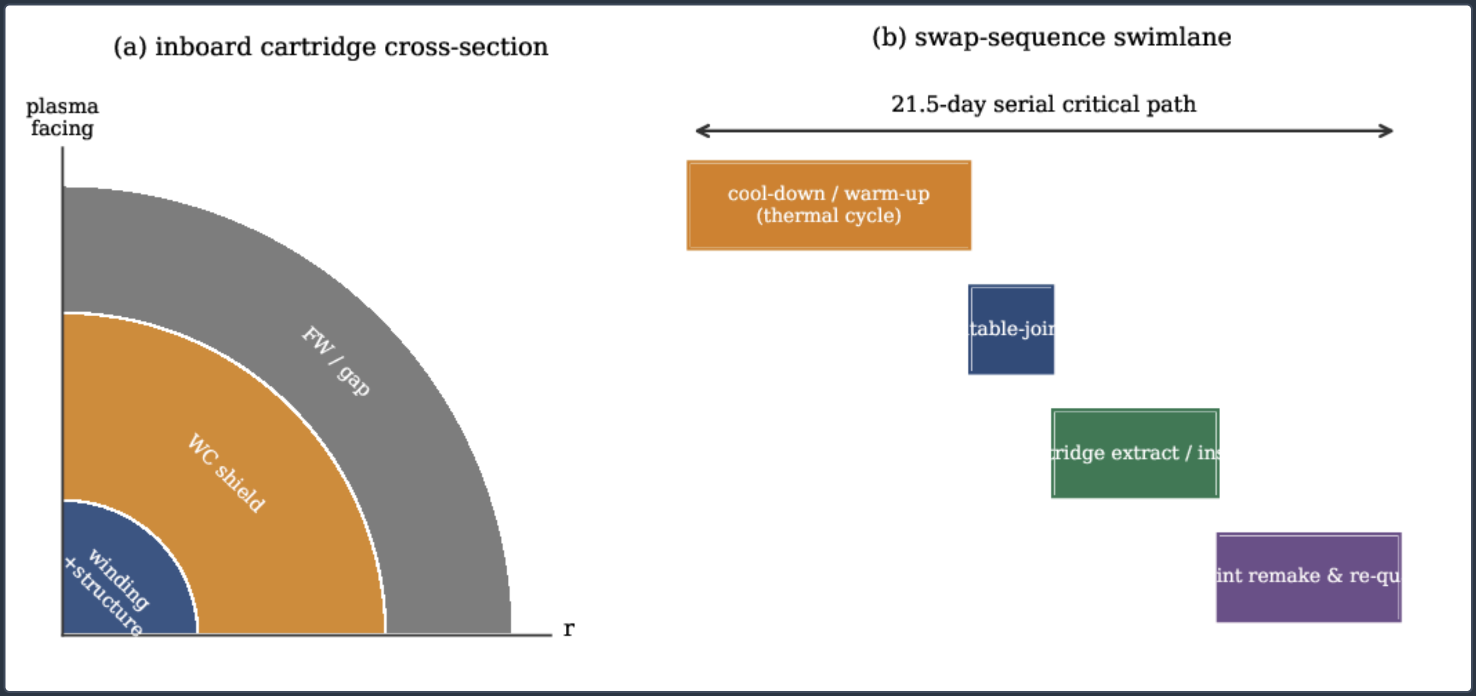

(Schematic.) (a) Inboard cartridge cross-section: winding-plus-structure, WC shield and first-wall/gap annuli inside the $R_0 - a$ envelope. (b) The serial swap swimlane: cool-down/warm-up (the dominant thermal term), demountable-joint break, cartridge extract/insert, and joint remake with re-qualification, summing to the **21.5**-day critical path.

§ 5

Discussion

AVAILABILITY AGAINST PUBLISHED BENCHMARKS

The honest headline is that the swap cadence pulls availability *below* the $\mathrm{CF}_0 = 0.69$ swap-free baseline at both operating points (Fig. 3). This is expected for a consumable core and is consistent with the availability envelopes discussed for tokamak plant systems and DEMO-class remote maintenance, where in-vessel maintenance is repeatedly identified as the dominant capacity-factor risk [24,25,22,23]. What distinguishes the consumable centrepost is that the availability-critical action is scheduled and its cadence is a computable function of neutron-damage physics, so it can be optimised in advance through 9 rather than mitigated reactively. In this sense the architecture converts an open reliability risk into a bounded design variable. Two comparators frame the **21.5**-day outage: it is short relative to a DEMO-class blanket-sector replacement but recurs far more often, and it is comparable to a light-water-reactor refuelling outage while occurring several times per full-power-year rather than once every **18**–**24** months. The consumable-core trade is therefore *cadence* against *duration*: the swap itself is fast, but its frequency, set by the short neutron life, is what governs. That is why the mid-current lever, which acts on frequency, dominates outage-duration surgery, which acts on the (already short) duration.

THE THROUGHPUT–AVAILABILITY TRADE

A quantitative honesty is required about the mid-current lever. Because it lowers P_{fus} from **85.04** to **70.28** MW while raising A from $\approx$ **0.586** to $\approx$ **0.643**, the time-averaged fusion power $A\,P_{\mathrm{fus}}$ moves from $\approx$ **49.8** to $\approx$ **45.2** MW — i.e. mid-current operation buys availability (continuity of service and fewer outages) at a modest cost in delivered power. Whether this is net-positive is a *mission* question, not a physics one: for a breeder valued on continuity of neutron and isotope service and on minimising in-vessel interventions, higher availability is the right objective; for a mission valued on peak source strength, the design point is preferred. We report both explicitly and take no economic position. The availability model 4 and the operating window 9 make either choice a transparent, pre-registered selection along the admissible current window rather than a hidden assumption.

FLEET IMPLICATIONS

The single-unit renewal model of §2.3 is the building block for fleet capacity factor. Because the swaps of independent units are asynchronous, a multi-unit fleet can partially mask individual outages, so the fleet capacity factor exceeds the single-unit availability by an amount that depends on the swap-cadence correlation and on spare-cartridge logistics. Propagating 4–6 to a four-unit fleet by time-domain Monte-Carlo is the subject of the fleet-availability companion [doi:10.5281/zenodo.22645951; https://www.kronosfusionenergy.com/publications/fleet-availability-under-consumable-centrepost-swap-cad.html], which uses the present single-unit model and outage distribution as its input. The cartridge-supply cadence implied by 6 — of order **40** columns over a **30**-year unit life at mid-current, and more per fleet — also feeds the critical-materials buildability analysis for REBCO tape and structural supply.

§ 6

Limitations

One item is genuinely open, and it is geometric: the inboard build (≈ 0.74 m) overruns the $R_0 - a = 0.72$ m envelope by ≈2 cm 8, to be closed by shield/winding re-optimization in 9. The structural (181 MPa, $6\times$ margin) and quench budgets already pass at the 16.84 T operating field, so the reconciliation is a bounded build-thickness adjustment rather than an open physics question. Two modelling caveats attach to the life numbers rather than to the operations conclusions: the centrepost "life" uses fast-fluence damage-limit proxies (10^{22}–10^{23} n m^{-2}, $E > 0.1$ MeV) rather than a full REBCO critical-current degradation curve, and the shield trade uses a 1-D infinite-cylinder CSG with a homogenized Cu + SS conductor proxy (no axial leakage, no port cut-outs). Both are conservative-leaning simplifications that tighten with tape-level and 3-D CAD-faithful neutronics; neither changes the qualitative operations picture, in which the swap governs availability and mid-current is the recovery lever.

§ 7

Conclusion

The consumable-centrepost architecture has a quantified, honest operations basis. A cartridge swap is a 21.5-day serial critical path dominated by cold-mass thermal cycling (8.5 d, $40\,\%$). Plant availability follows an alternating-renewal law $A = \mathrm{CF}_0/(1 + \mathrm{CF}_0\, t_{\mathrm{swap}}/T_{\mathrm{life}})$ that reproduces the frozen register anchors to ≤ 0.5 point: 0.582–0.590 at the design point and 0.638–0.648 at the mid-current point, a $\approx$ 5.7-point gain that is the architecture's primary availability lever, with a further $+0.8$–1.0 point from merged maintenance cadences. The elasticity identity $\partial \ln A/\partial \ln T_{\mathrm{life}} = -\partial \ln A/\partial \ln t_{\mathrm{swap}}$ shows that a fractional life gain and a fractional outage reduction are equally valuable, so mid-current operation dominates because its achievable fractional change ($+119\,\%$ in life) is far larger than the reach of thermal-term surgery ($-40\,\%$ in outage). The swap governs availability because the centrepost is neutron-lifetime bound ($0.21/0.46$ fpy), not stress-bound (181 MPa, $6\times$ margin) or quench-bound. The admissible operating-current window $[8.779, 9.656]$ MA makes the mid-current lever physically available, and the inboard radial build overruns the 0.72 m envelope by a bounded $\approx$2 cm to be closed by shield/winding re-optimization. The architecture is operations-ready with a single, well-posed geometry item to close.

Acknowledgments tocsectionAcknowledgments Part of the Kronos Fusion Energy 2026 design series. The author thanks the Kronos de-risking campaign for the frozen register serials underpinning this analysis and acknowledges the NVIDIA GPU HPC fleet on which the neutron-transport and reduced-order runs were executed.

Reproducibility. The 21.5-day swap critical path and 8.5-day thermal term, the availability figures (0.582–0.590 / 0.638–0.648), the neutron-lifetime bound (0.21 / 0.46 fpy), the 181 MPa / $6\times$ structural margin, the shield–life trade ($2.9 \times 10^{25} \to 1.7 \times 10^{23}$ n m^{-2} fpy^{-1} ; $0.003 \to 0.58$ fpy), the admissible current window ($[8.779, 9.656]$ MA), and the $\approx$2 cm radial overrun against $R_0 - a = 0.72$ m are frozen results of register serials BR-SX-18, BR-SX-16, BR-L1-A13b, BR-L1-A13, KX-L1-A21 and BR-SXD-06 in the Kronos Physics De-Risking Register (doi:10.5281/zenodo.22133057). The renewal-model and figure-generation script (`make_figs_2p104_swap_rami.py`) reproduces every panel and the frozen-anchor cross-check from these numbers. This paper is archived at its DOI (doi:10.5281/zenodo.22645931) and its official page is https://www.kronosfusionenergy.com/publications/operating-the-consumable-centrepost-of-a-compact-spheri.html.

Data availability tocsectionData availability This paper is archived at doi:10.5281/zenodo.22645931. The RAMI renewal model, availability computation, shield and operating-window tables, and radial-build reconciliation are archived with the deposit and reference the Kronos 2026 series and the de-risking register (doi:10.5281/zenodo.22133057). Any economic analysis is reported separately and is not included in the public deposit.

Competing interests tocsectionCompeting interests Provisional patent applications relating to aspects of this work have been filed. The author declares no other competing interests.

APPARATUS

Portfolio, People & Record

The intellectual-property estate, the people who built it, the limitations that gate it, and the sources it rests on.

1	4	40	27
GRANTED PATENT	2026 PROVISIONALS	TEAM MEMBERS	2022 PROVISIONALS

INTELLECTUAL PROPERTY

The patent portfolio

The estate spans a granted high-field magnet patent, pending utility and 2026 provisional filings that map to the two products, a digital-twin control provisional, a registered trademark application, and the original 2022 provisional family. Every patentable disclosure in the five-paper arXiv drop was protected **before** publication: the breeder and burner provisionals were filed 1–2 August, and a publication-gap omnibus filing the evening before the drop swept up the DEC, plasma-control, and REBCO-winding matter of the three otherwise-unprotected papers. Patent numbers and application serials are matters of public record; claim scope is summarised, not reproduced.

GRANTED & PENDING UTILITY

US 12,009,112	High-field tilted graded-REBCO magnet architecture (KRONO-002A) *· app. 17/878,550*	GRANTED
US 17/878,507	Core device / method (KRONO-001A) *· utility*	PENDING

2026 PROVISIONAL FILINGS — MAPPED TO THE PRODUCTS

64/124,209	Hyperion — spherical-tokamak tritium / helium-3 foundry *· breeder · filed Aug 2026*	FILED
64/124,220	Aegis / MetroVolt — synchrotron-cutoff, fuel-selection & plug-winding *· generator · filed Aug 2026*	FILED
64/115,167	KRONOS-CTRL digital-twin plant control *· provisional · filed Jul 2026*	FILED
64/005,440	Integrated spherical-tokamak fusion architecture *· early integrated-architecture filing · filed Mar 2026*	FILED
64/105,530	Negative-triangularity spherical-tokamak architecture *· foundational ST filing · filed Jul 2026*	FILED
64/128,097	Publication-gap omnibus — quasineutral two-species expander DEC · provenance-gated / latency-split plasma control · as-built high-field winding & conductor architecture *· filed 7 Aug 2026, the evening before the arXiv drop*	FILED

TRADEMARK & ORIGIN

FTK-98801894	Kronos Fusion Energy — trademark application	FILED
KR-2022-*	Original provisional family (KR-2022-00001 … 00027) *· 27 filings, 2022*	PRIORITY

The narrow, defensible magnet novelty — the specific conductor and the digital-twin winding optimisation, not high-field REBCO as a category — is the commercial core that can earn ahead of any Q > 1 milestone, with markets in fusion magnet supply, MRI/NMR, accelerators, and proton therapy. The claim is scoped honestly: the high field is a *system field* result, not a stand-alone-coil record; the small-bore plug coil is structurally infeasible as a bare winding but resolved by a stress-managed structural shield (feasible-pending-FEA); and the winding-tape experiment returned a *null result*. The value is the method, not a field record.

THE TEAM

Founding partners, board, advisors & auditors

Kronos is built by a bench of advanced-fuel-fusion, high-field-magnet, direct-conversion, and materials specialists, with a board and operations team drawn from defense, national laboratories, and industry. Dates are shown as ranges; where a tenure has ended or is term-ending, the range says so.

FOUNDING PARTNERS — SCIENCE

Dr. Gerald Kulcinski
Co-Founder · Helium-3 & Advanced-Fuel Fusion
UW–Madison · 2023–Present

Dr. Carl Weggel
Chief Scientist / S.M.A.R.T. Design
MIT Alcator Program · 2022–Present

Dr. Robert J. Weggel
Magnetic Field Design
MIT Magnet Lab · 2022–Present

BOARD

Priyanca Ford
Founder & CEO · Executive Board
2022–Present

Bandel Carano
Finance / Strategy
Oak Investment Partners / Stanford · 2025–2026

Patrick Schweiger
Fusion Device Engineering
Oklo / CFS / TerraPower · 2025–Present

SCIENTIFIC ADVISORS

Dr. Steven O. Dean
Fusion Policy & History
DOE / Fusion Power Associates · 2025–Present

Dr. Patrick H. Diamond
Plasma Turbulence & Transport
UC San Diego · 2025–Present

Dr. Jack J. Dongarra
HPC & Numerical Algorithms
Turing Award · 2025–Present

Dr. Nasr M. Ghoniem
Chief Material Scientist
UCLA · 2025–Present

Dr. Siegfried Glenzer
Plasma Physics & Laser Fusion
Stanford / SLAC · 2022–Present

Dr. David A. Hammer
Pulsed-Power Fusion
Cornell · 2025–Present

Dr. Donald A. Spong
Plasma Theory & Confinement
ORNL · 2025–Present

Dr. Curtis Smith
Risk Assessment & Nuclear PRA
MIT / Idaho National Lab · 2025–Present

RADM (Ret.) David Goggins
Naval Engineering & Power-Plant Design
U.S. Navy · 2023–2026

Dr. Konstantin Batygin
Mathematician
Caltech · 2022–2025

Dr. Ruben Fair
Magnet Design / ITER Liaison
PPPL / Jefferson Lab · 2022–2025

Dr. Paul S. Weiss
Materials & Nanotechnology
UCLA · 2022–2025

SCIENTIFIC AUDITORS

Dr. Wilfred A. Cooper
Plasma Equilibrium Theory
EPFL / Swiss Plasma Center · 2025–Present

Dr. Ahmed Hassanein
Plasma–Material Interactions
Purdue / Argonne · 2025–Present

Dr. Patrick E. Hopkins
Extreme Thermal Materials
U. of Virginia · 2025–Present

Dr. Peter Hosemann
Materials Joining & Structural Integrity
UC Berkeley · 2025–Present

Dr. Travis W. Knight
Advanced Nuclear Fuels & Systems
U. of South Carolina · 2025–Present

Dr. Philippe Lebrun
Cryogenics & Magnet Cooling
CERN · 2025–Present

Dr. Nitendra Singh
Nuclear Safety & Fuel Cycle
ITER · 2025–Present

Dr. Guido Van Oost
Magnetic Confinement & Fusion Systems
Ghent University · 2025–Present

Dr. Gary S. Was
Radiation Materials & Structural Integrity
U. of Michigan · 2025–Present

Dr. Ray Sedwick
Direct Energy Conversion
U. of Maryland · 2025

OPERATIONS

Michael Laughlin
Chief Operating Officer
2022–Present

Martin Owens
Chief Strategy Officer
LANL / GE Hitachi · 2022–Present

MG (Ret.) Paul Pardew
Chief Contracting Officer
Army Contracting Command · 2022–Present

David Beck
Fusion Commercialization
U.S. Space Force · 2024–Present

Sushma Bhatia
Environmental & Legislative
Google · 2022–Present

Michael De Frenza
Technology Licensing
2023–Present

MG (Ret.) Robin L. Fontes
Cybersecurity & Defense
Army Cyber Command · 2022–Present

Vijay Gehani
Supply Chain & Components
INOX India · 2024–Present

Jon Michel Greenwood
IT & AI Infrastructure
Live Nation · 2023–Present

Brian C. O'Neill
National Security
CIA / ODNI · 2022–Present

Gen. (Ret.) Gustave F. Perna
DoD Liaison
Operation Warp Speed · 2022–2023

Andrea Romero
Marketing Lead
2022–Present

Legal counsel is retained; those roles are held on the internal roster and are not listed here.

SOURCES

References

1 J E Menard *et al*, Fusion nuclear science facilities and pilot plants based on the spherical tokamak, *Nucl. Fusion* **56** 106023 (2016). doi:10.1088/0029-5515/56/10/106023

2 A E Costley, J Hugill and P F Buxton, On the power and size of tokamak fusion pilot plants and reactors, *Nucl. Fusion* **55** 033001 (2015).

3 A Sykes *et al*, Compact fusion energy based on the spherical tokamak, *Nucl. Fusion* **58** 016039 (2018).

4 J E Menard *et al*, Overview of the physics and engineering design of NSTX Upgrade, *Nucl. Fusion* **52** 083015 (2012).

5 B N Sorbom *et al*, ARC: a compact, high-field, fusion nuclear science facility and demonstration power plant with demountable magnets, *Fusion Eng. Des.* **100** 378 (2015). doi:10.1016/j.fusengdes.2015.07.008

6 D G Whyte, J Minervini, B LaBombard, E Marmar, L Bromberg and M Greenwald, Smaller & sooner: exploiting high magnetic fields from new superconductors for a more attractive fusion energy development path, *J. Fusion Energy* **35** 41 (2016). doi:10.1007/s10894-015-0050-1

7 A J Creely *et al*, Overview of the SPARC tokamak, *J. Plasma Phys.* **86** 865860502 (2020). doi:10.1017/S0022377820001257

8 S Hahn *et al*, 45.5-tesla direct-current magnetic field generated with a high-temperature superconducting magnet, *Nature* **570** 496 (2019). doi:10.1038/s41586-019-1293-1

9 J L MacManus-Driscoll and S C Wimbush, Processing and application of high-temperature superconducting coated conductors, *Nat. Rev. Mater.* **6** 587 (2021). doi:10.1038/s41578-021-00290-3

10 A Molodyk *et al*, Development and large volume production of extremely high current density $YBa_2Cu_3O_7$ superconducting wires for fusion, *Sci. Rep.* **11** 2084 (2021).

11 P Bruzzone *et al*, High temperature superconductors for fusion magnets, *Nucl. Fusion* **58** 103001 (2018).

12 Y Iwasa, *Case Studies in Superconducting Magnets: Design and Operational Issues*, 2nd ed. (Springer, New York, 2009).

13 P K Romano, N E Horelik, B R Herman, A G Nelson, B Forget and K Smith, OpenMC: a state-of-the-art Monte Carlo code for research and development, *Ann. Nucl. Energy* **82** 90 (2015). doi:10.1016/j.anucene.2014.07.048

14 D A Brown *et al*, ENDF/B-VIII.0: the 8th major release of the nuclear reaction data library with CIELO-project cross sections, new standards and thermal scattering data, *Nucl. Data Sheets* **148** 1 (2018). doi:10.1016/j.nds.2018.02.001

15 M J Norgett, M T Robinson and I M Torrens, A proposed method of calculating displacement dose rates, *Nucl. Eng. Des.* **33** 50 (1975). doi:10.1016/0029-5493(75)90035-7

16 K Nordlund *et al*, Improving atomic displacement and replacement calculations with physically realistic damage models, *Nat. Commun.* **9** 1084 (2018). doi:10.1038/s41467-018-03415-5

17 S J Zinkle and G S Was, Materials challenges in nuclear energy, *Acta Mater.* **61** 735 (2013).

18 G S Was, *Fundamentals of Radiation Materials Science: Metals and Alloys*, 2nd ed. (Springer, Berlin, 2017).

19 M R Gilbert, S L Dudarev, S Zheng, L W Packer and J-Ch Sublet, An integrated model for materials in a fusion power plant: transmutation, gas production, and helium embrittlement under neutron irradiation, *Nucl. Fusion* **52** 083019 (2012).

20 D X Fischer *et al*, The effect of fast neutron irradiation on the superconducting properties of REBCO coated conductors, *Supercond. Sci. Technol.* **31** 044006 (2018).

21 M Kovari *et al*, PROCESS: a systems code for fusion power plants — Part 1: physics, *Fusion Eng. Des.* **89** 3054 (2014). doi:10.1016/j.fusengdes.2014.09.018

22 G Federici *et al*, Overview of the DEMO staged design approach in Europe, *Nucl. Fusion* **59** 066013 (2019).

23 M Abdou, N B Morley, S Smolentsev *et al*, Blanket/first wall challenges and required R&D on the pathway to DEMO, *Fusion Eng. Des.* **100** 2 (2015).

24 T Pinna, R Boullon, C Cortes, G Dell'Orco *et al*, Reliability, availability, maintainability and inspectability (RAMI) analyses of ITER

COLOPHON

How this document was made

The Kronos Fleet — Combined Editorial, 2026 is set in **Fraunces** (display), **Gelasio** (text), and **IBM Plex Mono** (data & equations), carried forward from the Kronos editorial design system.

The figures are rendered at 300 dpi from the deposited generator scripts; the document is composed as a single self-contained file with embedded fonts and imagery, paginated to US Letter, and rendered to PDF through a headless Chromium engine in matched light and dark editions.

Every headline quantity carries an evidence class; withdrawn and restated values are marked as such. Nothing herein is frozen beyond the founder-approved Tier-A set.

Explore it live — turn the interactive 3-D model, run the deposited solvers in the physics validator, and watch the companion film series.

LEGAL NOTICE

Notice, status, and distribution

Conceptual design & simulation study. This document reports a conceptual design and simulation study. It is not a construction commitment, a safety-analysis report, a regulatory filing, or an offer of securities. Forward-looking statements — schedules, costs, market sizes, and performance — are estimates subject to the limitations set out in the Simulations part and may change.

Numbers and their classes. Quantities are reported with evidence classes and case labels; modelled, assumed, and requirement-class values are identified as such and are not to be quoted without their labels.

Public edition. This edition carries the physics and design only; all financial, funding, and defense-commercial content has been removed for public distribution. The scientific text corresponds to the arXiv and journal submissions.

THE 2026 KRONOS SERIES

One programme, many papers

This editorial is one paper in the Kronos 2026 series — a real fusion company's complete, reproducible physics record for a spherical-tokamak breeder and its low-neutron D–^{3}He tandem-mirror burners. Every headline number is a frozen anchor in the Physics De-Risking Register.

Explore the whole programme: the De-Risking Register, the interactive 3-D model, and the physics validator.

KRONOS FUSION ENERGY

Operating the Consumable Centrepost of a Compact Spherical-Tokamak Breeder: Demountable-Cartridge Swap Logistics, Fleet RAMI, and Centrepost Radial-Budget Reconciliation

A real fusion company building real machines. Explore the science, live.

Zenodo · doi:10.5281/zenodo.22645931

Read on kronosfusionenergy.com

The Physics De-Risking Register